LEVEL II

AD A102178

PSR Report 1016

LIDARS FOR SMOKE AND DUST CLOUD DIAGNOSTICS

S. F. Fujimura
R. E. Warren
R. F. Lutomirski

November 1980

DTIC ELECTE JUL 29 1981 S D F

Final Report
Contract DAAK20-79-C-0040

Sponsored by
U.S. Army Night Vision and
Electro-Optics Laboratory
Laser Division
Fort Belvoir, Virginia 22060

PACIFIC·SIERRA RESEARCH CORP.
1456 Cloverfield Blvd. • Santa Monica, California 90404

81 7 29 030

PSR Report 1016

LIDARS FOR SMOKE AND DUST CLOUD DIAGNOSTICS

S. F. Fujimura
R. E. Warren
R. F. Lutomirski

November 1980

Final Report
Contract DAAK20-79-C-0040

Sponsored by
U.S. Army Night Vision and
Electro-Optics Laboratory
Laser Division
Fort Belvoir, Virginia 22060

PACIFIC·SIERRA RESEARCH CORP.
1456 Cloverfield Blvd. • Santa Monica, California 90404

SECURITY CLASSIFICATION OF THIS PAGE (When Data Entered)

REPORT DOCUMENTATION PAGE

READ INSTRUCTIONS BEFORE COMPLETING FORM

1. REPORT NUMBER: PSR Report-1016	2. GOVT ACCESSION NO.: AD-A102 178
3. RECIPIENT'S CATALOG NUMBER:	
4. TITLE (and Subtitle): LIDARS FOR SMOKE AND DUST CLOUD DIAGNOSTICS.	5. TYPE OF REPORT & PERIOD COVERED: Final Report, 9/79 – 6/80
	6. PERFORMING ORG. REPORT NUMBER: PSR Report 1016
7. AUTHOR(s): S. F. Fujimura, R. E. Warren, R. F. Lutomirski	8. CONTRACT OR GRANT NUMBER(s): DAAK20-79-C-0040
9. PERFORMING ORGANIZATION NAME AND ADDRESS: Pacific-Sierra Research Corporation, 1456 Cloverfield Blvd., Santa Monica, California 90404	10. PROGRAM ELEMENT, PROJECT, TASK AREA & WORK UNIT NUMBERS: Project 1L162709DH95
11. CONTROLLING OFFICE NAME AND ADDRESS: USERADCOM, Fort Monmouth, New Jersey 07703	12. REPORT DATE: November 1980
	13. NUMBER OF PAGES: 31
14. MONITORING AGENCY NAME & ADDRESS (if different from Controlling Office): Dir., NV Electro-Optics Laboratory, Laser Division, Attn: DELNV-L, Ft. Belvoir, Virginia 22060	15. SECURITY CLASS. (of this report): UNCLASSIFIED
	15a. DECLASSIFICATION/DOWNGRADING SCHEDULE:

16. DISTRIBUTION STATEMENT (of this Report)

17. DISTRIBUTION STATEMENT (of the abstract entered in Block 20, if different from Report)

18. SUPPLEMENTARY NOTES

19. KEY WORDS (Continue on reverse side if necessary and identify by block number)

Battlefield dust and smoke	Dust model
Optical transmission	Lidar transmission
Particulates	Electro-optical propagation

20. ABSTRACT (Continue on reverse side if necessary and identify by block number)

An algorithm that integrates a time-resolved lidar signature for use in estimating transmittance, extinction coefficient, mass concentration, and CL values generated under battlefield conditions is applied to lidar signatures measured during the DIRT-I tests. Estimates are given for the dependence of the inferred transmittance and extinction coefficient on uncertainties in parameters such as the obscurant backscatter-to-extinction ratio. The enhanced reliability in estimating transmittance through use of a target behind the

DD FORM 1 JAN 73 1473 EDITION OF 1 NOV 65 IS OBSOLETE

SECURITY CLASSIFICATION OF THIS PAGE (When Data Entered)

BLOCK 20 (cont.)

obscurant cloud is discussed. It is found that the inversion algorithm can produce reliable estimates of smoke or dust transmittance and extinction from all points within the cloud for which a resolvable signal can be detected, and that a single point calibration measurement can convert the extinction values to mass concentration for each resolvable signal point.

PREFACE

This report was prepared for the U.S. Army Night Vision and Electro-Optics Laboratory, Laser Division, Fort Belvoir, Virginia. It constitutes Pacific-Sierra Research Corporation's final report on contract DAAK20-79-C-0040 with that agency. An earlier version was presented as a paper to the Fourth Smoke/Obscurants Symposium, held 22-23 April 1980 at Harry Diamond Laboratories, Adelphi, Maryland.

SUMMARY

This report develops an algorithm for inferring the absolute transmittance and extinction coefficient throughout an obscurant cloud from which a resolvable signal can be detected, using only relative ambient and cloud lidar signatures. Simple expressions are derived to approximate the errors in the inferred values for given uncertainties of the cloud parameter. The obscurant mass concentration and concentration path integral (CL values) are shown to be proportional to the extinction coefficient, so that relative values of mass concentration and CL values can be directly inferred from the extinction coefficient. A point calibration measurement is needed to infer absolute values, however.

The results are applied to actual field data for dust clouds measured during the DIRT-I experiment.

CONTENTS

FIGURES

I. INTRODUCTION

Work performed under a previous contract [Warren and Lutomirski, 1979] established the validity of an algorithm that inverts lidar signatures for use in characterizing the aerosol dynamics of obscurant clouds under battlefield conditions. The algorithm integrates a time-resolved lidar signature to estimate (1) transmittance, (2) extinction coefficient, (3) mass concentration, and (4) concentration path integral (CL value) for spatially varying obscurant clouds. In the earlier study, computer simulations of the lidar return used to test the algorithm's sensitivity to noise and parameter uncertainties (such as in the backscatter-to-extinction ratio) showed that locally measuring the scattering properties of the obscurant cloud would allow the mass concentration and CL values to be inferred throughout the obscurant cloud where the lidar return is above the noise.

The present effort establishes the feasibility of inferring the transmittance and the extinction coefficient throughout the cloud using only the ambient and obscurant cloud lidar signatures, without additional point calibration measurements. We find that the required normalization can be accomplished by using the ambient signature and either waiting until the cloud is tenuous or having a scanning capability to probe the region behind the cloud. A target behind the cloud is useful for enhancing the reliability of the normalization, but is not essential. The relative mass concentration and CL value of an obscurant cloud can be inferred directly from the extinction coefficient. The absolute mass concentration and CL value can be found, if needed, by performing a single point measurement along the lidar path within the cloud. Directly measuring the concentration instead of measuring the particle size distribution is preferable for that purpose.

Applying the above method to lidar signatures from dust clouds measured during the DIRT-I tests [van der Laan, 1979], sample calculations show maximum errors of less than 5 percent in transmittance and less than 20 percent in the extinction coefficient for a 10 percent

uncertainty in the inferred scattering parameters. For the same uncertainty in the scattering parameters, the errors in the concentration and the CL value are less than 20 percent and 12 percent, respectively. The report establishes that simple equations can predict these errors.

Section II defines the assumptions for the model and derives expressions for the transmittance and extinction of the cloud, giving solution methods with or without a point measurement. Section III investigates the sensitivity of the algorithm to uncertainties in the obscurant cloud backscatter-to-extinction ratio α_s and derives simple closed-form estimates for the uncertainty in the estimated transmittance and extinction coefficient.

Section IV calculates the concentration and CL values of the smoke or dust (hereafter simply *smoke*) and recommends an alternative to obtaining local measurements of the particle number distribution. Section V applies the inversion algorithm to data taken during DIRT-I, numerically calculating the transmittance, extinction coefficient, mass concentration, and CL values and estimating the ranges of possible errors. Section VI summarizes the proposed model and the results of applying the algorithm to the DIRT-I data.

The need for a practical approach to deriving detailed information on the spatial and temporal dynamics of battlefield obscurants is well established. An additional strong motivation for the analysis described here is the concurrent development by the Army Night Vision and Electro-Optics Laboratory of a two-color, three-dimensional scanning lidar. The added flexibility of that system substantially enhances the usefulness of the inversion algorithm in that the required transmittance normalization can be performed by selecting an optimal combination of spatial scan, wavelength, and temporal signature. The work here represents a step toward exploiting this improved capability for inferring smoke/dust dynamics in the field.

II. ALGORITHM FOR ESTIMATING OBSCURANT TRANSMITTANCE AND EXTINCTION

The formal solution to the radiative transport equation for a spatially varying medium was solved for a general scattering medium by Warren and Lutomirski [1979]. Their solution can be specialized to lidars, resulting in the single-scattering lidar equation

$$P(z) = \frac{A\beta(z)T^2(z)}{G(z)} \exp\left(\frac{-b^2}{G(z)}\right), \tag{1}$$

where $P(z)$ is the instantaneous backscatter power received at time t [proportional to the range $z(t = 2z/c)$] and A is a constant for given lidar parameters--which include wavelength of the lidar laser, losses or efficiency of the transmitting and receiving optics, effective receiver aperture, backscatter phase function, and a dimensional constant. The backscatter coefficient at range z is given by $\beta(z)$; the one-way transmittance of the medium to range z is given by $T(z)$. The two-way, round-trip transmittance of the medium to range z, $T^2(z)$, can be written as

$$T^2(z) = \exp\left[-2\int_0^z dz'\varepsilon(z')\right], \tag{2}$$

where $\varepsilon(z)$ is the extinction coefficient at range z. The center-to-center separation of the transmitter and receiver is b, and

$$G(z) = a_R^2 + \theta_R^2 z^2 + (a_T + \theta_T z)^2, \tag{3}$$

where a_R is the receiver aperture radius, θ_R is the field-of-view half-angle, a_T is the transmitter aperture radius, and θ_T is the transmitter beam divergence half-angle. Equation (3) assumes a Gaussian aperture and a Gaussian field-of-view receiver.

Equation (1), the lidar equation, is valid as long as the transmitter has a short pulse (less than a few hundred nanoseconds) and a narrow beam width (at most a few centimeters); a small divergence (on the order of a few milliradians) is required for there to be no significant transverse variations in the lidar backscatter power return. The receiver field-of-view must be narrow (on the order of a few milliradians) to minimize the effects of multiple scattering.

The lidar backscatter power return from a smoke cloud raised by an explosion is composed of two parts--the ambient air and the smoke cloud return. The cloud usually comprises a range of particle sizes describable by a particle size distribution $n(r, z)$, where r is the radius of the particle. In what follows, the subscript a refers to ambient air, s to smoke particles only, and c to ambient air and smoke combined.

To use Eq. (1), we make several assumptions about the backscatter and extinction coefficients. First, we assume that the ambient air backscatter coefficient β_a and extinction coefficient ε_a are constant throughout the range and are unaffected by the smoke. In other words, the partial volume occupied by the smoke is small and the relaxation time for β_a due to the explosion of the smoke is fairly short, so that β_a and ε_a return to their equilibrium values soon after the explosion.

Second, we assume that for the ambient air where the coefficients are constant, $\beta_a = \alpha_a \varepsilon_a$. As shown in Fenn [1966], the relationship between the extinction and backscatter coefficients is

$$\beta = \alpha \varepsilon^{\ell} , \tag{4}$$

where both α and ℓ are constants. Since the lidar equation [Eq. (1)] is for the single-scattering model, ℓ is taken to be 1, giving a linear relationship between the backscatter and the extinction coefficients.

Finally, we assume that $n_s(r, z, t)$--the number of smoke particles with radius r, range z, and time t--is separable, such that

$$n_s(r, z, t) = n_{1s}(r) n_{2s}(z, t) , \tag{5}$$

and that the particle size distribution is constant. The total number of particles per unit volume $n_{2s}(z, t)$ may vary with range and time, which will cause $\varepsilon_s(z)$ to so vary. That assumption allows expressing the smoke backscatter coefficient as $\beta_s(z) = \alpha_s \varepsilon_s(z)$, where α_s is independent of range and time.

The lidar backscatter power return in ambient air is

$$P_a(z) = \frac{A\beta_a T_a^2(z)}{G(z)} \exp\left(\frac{-b^2}{G(z)}\right) ; \tag{6}$$

in the presence of smoke, the total backscatter power return becomes

$$P_c(z) = \frac{A\beta_c(z) T_c^2(z)}{G(z)} \exp\left(\frac{-b^2}{G(z)}\right) . \tag{7}$$

The backscatter and extinction coefficients for combined ambient air and smoke consist of the sum of the component coefficients:

$$\beta_c(z) = \beta_a + \beta_s(z) ; \quad \varepsilon_c(z) = \varepsilon_a + \varepsilon_s(z) . \tag{8}$$

Combining Eqs. (7) and (8) results in the following relation for $T_c^2(z)$:

$$T_c^2(z) = T_a^2(z) T_s^2(z) . \tag{9}$$

Dividing Eq. (7) by Eq. (6) and substituting the expressions for β_c and T_c^2 gives

$$\frac{P_c(z)}{P_a(z)} = T_s^2(z) + \frac{\beta_s(z)}{\beta_a} T_s^2(z) . \tag{10}$$

Note that no explicit knowledge of the actual lidar parameters (such as wavelength, transmitter or receiver aperture, efficiency of the lidar pulse, power) is necessary; all such information is carried in the ambient backscatter signature P_a. A Gaussian aperture and field of view were assumed for G(z), but since G(z) cancels, Eq. (10) is now valid for more general problems--that is, those that have the form of Eq. (1).

The transmittance of the smoke $T_s^2(z)$ can be differentiated with respect to z. Substituting $\beta_s(z)/\alpha_s$ for $\varepsilon_s(z)$ then gives an expression for $\beta_s(z)$:

$$\beta_s = \frac{\alpha_s}{2T_s^2(z)} \left(- \frac{dT_s^2(z)}{dz} \right) , \tag{11}$$

and substituting Eq. (11) into Eq. (10) gives a first-order differential equation for T_s^2:

$$\frac{P_c(z)}{P_a(z)} = T_s^2(z) + \frac{\alpha_s}{2\beta_a} \left(- \frac{dT_s^2(z)}{dz} \right) , \tag{12}$$

which can be integrated to yield

$$T_s^2(z) = \left[\exp\ (qz) \right] \left[1 - q \int_0^z \frac{P_c(z')}{P_a(z')} \exp\ (-qz')\ dz' \right] , \tag{13}$$

where $q \equiv 2\beta_a/\alpha_s$ and $T_s^2(0) = 1$. Range zero ($z = 0$) can be chosen arbitrarily--but, for simplicity, it should be chosen so that $z = 0$ is in a region in front of the smoke cloud, i.e., where $P_c(z) = P_a(z)$. Thus, the exact position of the lidar is not needed for the calculation of $T_s^2(z)$. Once $T_s^2(z)$ has been calculated, Eq. (10) can be solved for the backscatter coefficient; substituting for β_s, the extinction coefficient at range z is

$$\varepsilon_s(z) = \frac{q}{2}\left[\frac{P_c(z)}{P_a(z)T_s^2(z)} - 1\right] . \qquad (14)$$

The smoke cloud data usually consist of the range-resolved amplitude of the backscatter power return taken at predetermined time intervals, beginning before the smoke cloud is introduced and lasting until it dissipates. Figure 1 shows the 10.6 μm backscatter data from event F-6 during DIRT-I. The range (in meters) is given along the abscissa, and the log of the backscatter amplitude, along the ordinate. At T = 0, the spike at 100 m is due to a reflector used to calibrate the range; the spike at 2000 m is a target used to calibrate the range and measure transmittance. The ambient air backscatter amplitude $P_a(z)$ is shown in the T = 0 frame. In the next frame, T + 19s, detonation of the explosive has already occurred, causing an extremely dense cloud at 1000 m; there is therefore little penetration of the laser beam into the cloud, and the target at 2000 m is completely obscured. As time passes, there is greater penetration until the cloud is tenuous enough to allow the laser beam to pass through, and the backscatter amplitude from the target behind the cloud becomes visible.

The smoke cloud data give $P_a(z)$ and $P_c(z)$, but a value for q must be obtained to solve for the smoke transmittance and the extinction coefficient. There are two main methods. Method I is to take a local point measurement of q along the path of propagation of the lidar beam. Method IIa is to pick a set of backscatter amplitude data in which the smoke is prevalent but the backscatter amplitude of the ambient air from behind the cloud is both visible and well above the noise level. Far beyond the smoke cloud, where $z = z_{ns}$, there is essentially no smoke; so the extinction coefficient for the smoke $\varepsilon_s(z_{ns})$ is zero in that region, and the ratio $P_c(z_{ns})/P_a(z_{ns})$ is constant. From either Eq. (12) or Eq. (14) it follows that $P_c(z_{ns})/P_a(z_{ns})$ equals $T_s^2(z_{ns})$ in the region beyond the smoke cloud. Thus, the value of q can be found by varying q in Eq. (13) until $T_s^2(z)$ equals $T_s^2(z_{ns})$. An alternative method (IIb) is to place a target in the smoke-free region beyond

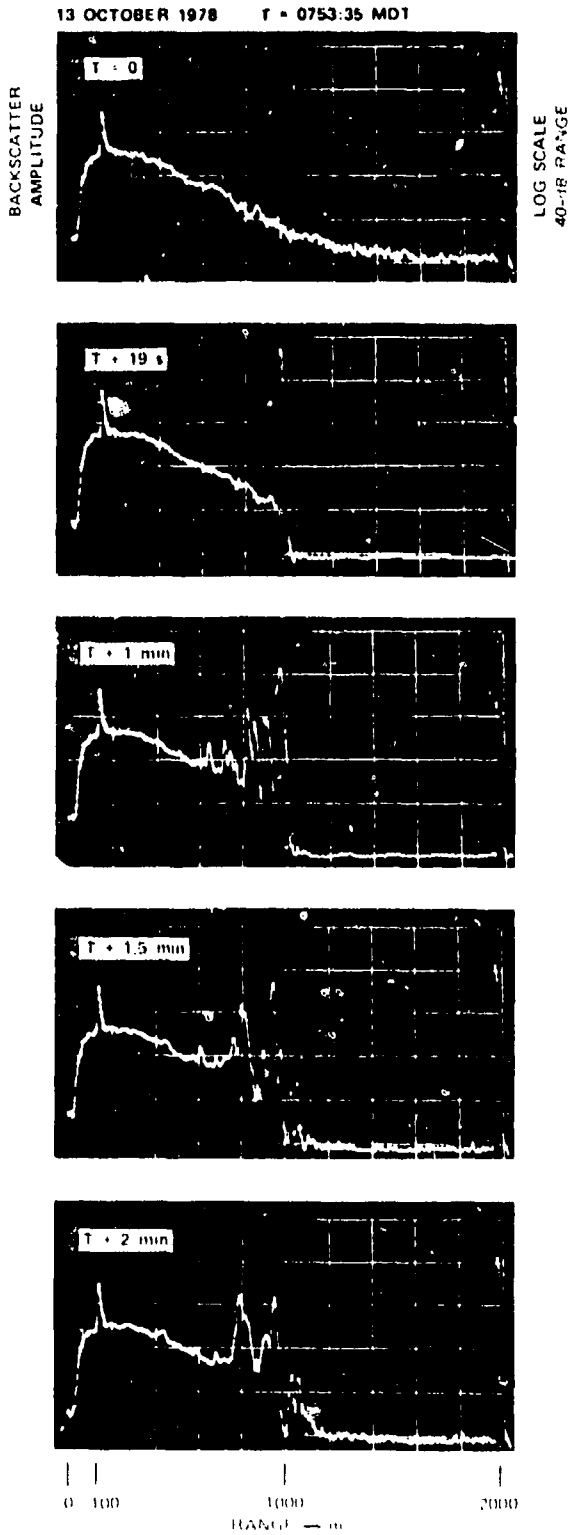

Fig. 1--Event F-6 10.6 μm backscatter data. Data from DIRT-I [van der Laan, 1979].

the smoke cloud in line with the laser beam. The ratio of the backscatter amplitude of the target in ambient air (R_a) to the backscatter amplitude of the target with the smoke cloud when the target is clearly visible (R_c) is just $T_s^2(z_t)$, where z_t is the target range, i.e., $T_s^2(z_t) = R_c/R_a$.

The T_s^2 found either way should result in identical values, but method IIb will improve the accuracy of T_s^2 due to the higher signal-to-noise ratio (SNR) of the target backscatter data. The value of T_s^2 can be substituted into Eq. (13) and combined with $P_c(z)$ and $P_a(z)$ to iterate for a value of q. In the lidar equation, P(z) is in absolute units such as watts, but by using the ratio of P_c to P_a, only the relative values of P_c and P_a are needed to solve for the smoke transmittance and the extinction coefficient. Also note that if the value for β_a is known, methods IIa and IIb supply a technique to find the value of α_s remotely.

If q is constant for a given smoke cloud, then once the value of q has been found, $T_s^2(z)$ and $\varepsilon_s(z)$ can be calculated for all times over which the backscatter data are taken. If the point measurement method is used, $T_s^2(z)$ and $\varepsilon_s(z)$ can be calculated for very dense clouds up to the deepest point of penetration of the laser beam; while with method IIa or IIb, the cloud has to dissipate so that backscatter data can be collected from beyond it. If the lidar is capable of scanning the cloud horizontally or vertically, then either method I or method IIa can find q when the central region of the cloud is too dense for the laser beam to penetrate. By method I, q can always be found. A scanning lidar can collect backscatter data from behind the less dense edges of the cloud where there is no smoke. Then q can be calculated by method IIa and the remainder of the cloud can be scanned to obtain a three-dimensional estimate of $T_s^2(z)$ and $\varepsilon_s(z)$ for all points from which a signal above the noise level is received.

III. SENSITIVITY ANALYSIS OF THE TRANSMITTANCE AND THE EXTINCTION COEFFICIENT

The transmittance and the extinction coefficient were calculated in Eqs. (13) and (14). Both functions are dependent on the range z, but errors in range are usually minimal. (Note that range and time resolution are related by $\Delta t = 2\Delta z/c$, so that a 10 m range resolution requires a 60 ns time resolution in the recorded lidar signal.) Ignoring errors due to range, the uncertainty in the transmittance is due to noise in the backscatter power returns of the ambient air and smoke cloud (P_a and P_c) and the coefficient q. In Warren and Lutomirski's [1979] work on simulated lidar signals with superimposed Gaussian noise, numerical computer output showed that the noise-averaging produced by the integration for transmission gives reasonably correct results for low SNRs--for example, for short-range transmittance of signals having an SNR $\gtrsim$ .1. The major source of error for the transmittance is therefore determining q. Differentiating the expression for transmittance with respect to q gives an expression for the uncertainty:

$$\frac{\Delta T_s}{T_s} = \frac{\Delta q}{2q}\left[1 - \frac{e^{qz}}{T_s^2} + qz + \frac{q}{T_s^2}\int_0^z \frac{P_c(z')}{P_a(z')}\, qz'\, e^{q(z-z')}\, dz'\right] . \qquad (15)$$

Equation (15) is difficult to apply, but for regions where $qz \ll 1$,

$$\frac{\Delta T_s}{T_s} \approx \frac{\Delta q}{q}\left(\frac{T_s^2 - 1}{2T_s^2}\right) . \qquad (16)$$

Figure 2 plots Eq. (16) for various values of T_s. The estimate of T_s is not very sensitive to errors in q for large values of T_s. For small values (which correspond to denser clouds), T_s becomes much more sensitive to errors in q, implying that for dense clouds, local measurements

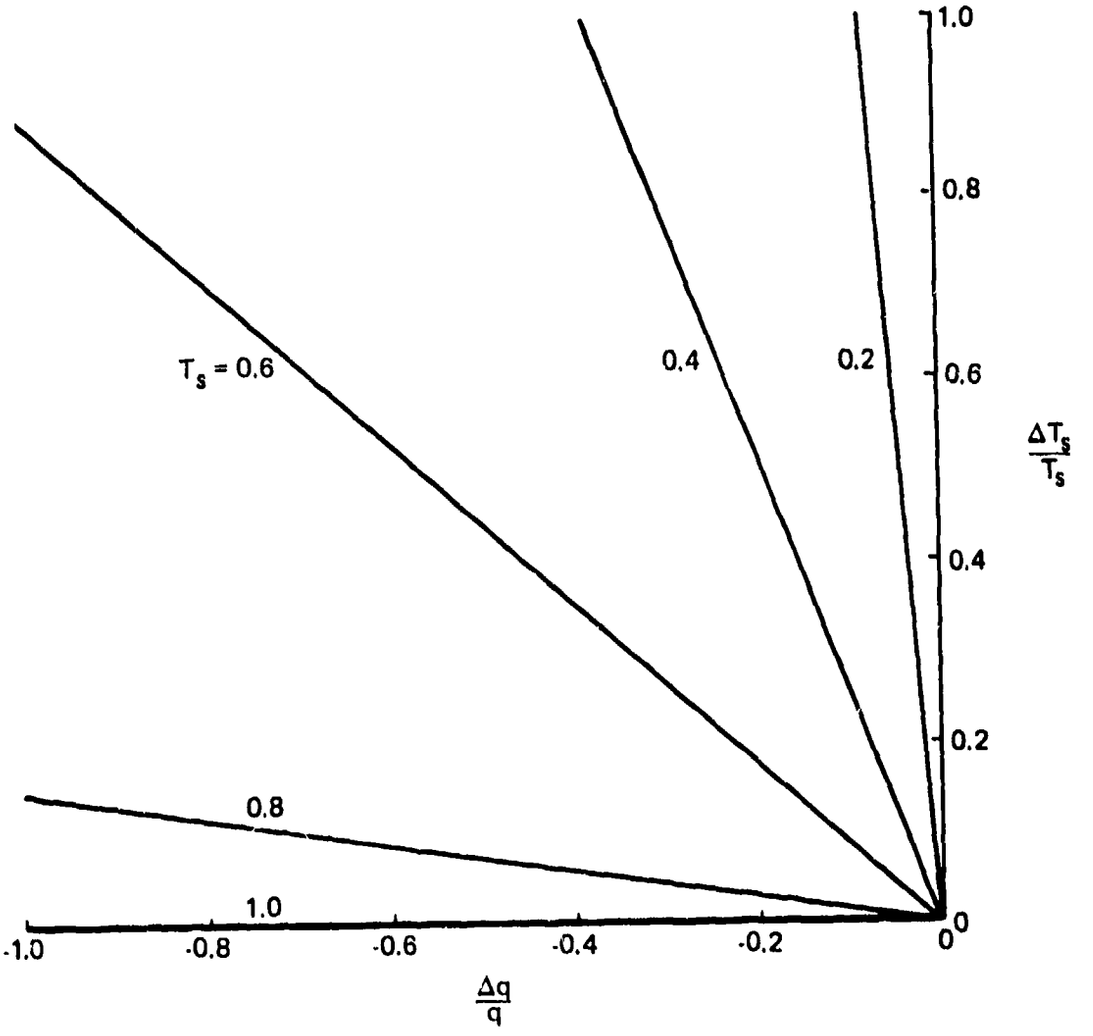

Fig. 2--Effect of error in q on estimated transmittance

of q may be necessary to minimize uncertainty in q. For example, in a dense cloud where the one-way transmittance of the smoke is only .25 and the acceptable error in T_s is 10 percent, the allowable error in q is about 1 percent.

The errors for the extinction coefficient are more serious than those for the transmittance. As Eq. (14) shows, there is no integral to average out noise in the backscatter power return. Any noise in the signal will hence directly affect the result for ε_s; the problem will increase with denser clouds and longer ranges, due to the low SNR. Compounding the problem is the uncertainty in q. From Eq. (14), the uncertainty in ε_s is

$$\frac{\Delta\varepsilon_s}{\varepsilon_s} = \frac{\Delta q}{q}\left\{1 - \left(1 + \frac{q}{2\varepsilon_s}\right)\left[1 - \frac{e^{qz}}{T_s^2} + qz + \frac{q}{T_s^2}\int_0^z \frac{P_c(z')}{P_a(z')}\, qz'\, e^{q(z-z')}\, dz'\right]\right\}. \tag{17}$$

The behavior of Eq. (17) is clarified by assuming $qz \ll 1$; then

$$\frac{\Delta\varepsilon_s}{\varepsilon_s} \simeq \frac{\Delta q}{q}\left[\frac{1}{T_s^2} - \frac{q}{2\varepsilon_s}\left(\frac{1 - T_s^2}{T_s^2}\right)\right]. \tag{18}$$

Equation (18) shows that the estimates for the extinction coefficient are good for larger values of the smoke transmittance. The second term in Eq. (18) is a major source of error only when ε_s is very small ($\ll \Delta q$).

The quantity ε_s is very small mainly in two regions--in front of and behind the smoke cloud; inside the cloud, it is usually much larger than Δq. In front of the smoke cloud, T_s^2 equals unity, so the second term vanishes. Beyond the cloud, ε_s theoretically returns to zero; but because ε_s is calculated from signals that have traveled through the cloud, the SNR is very low, the estimate of ε_s will suffer large uncertainties, and the second term can become large. Errors of a few orders of magnitude for ε_s beyond the cloud are not unexpected; but since ε_s is near zero, the absolute effect is minor.

Figure 3 plots the dominant contribution of the error in the estimates of the extinction coefficient due to the uncertainty in q. Comparison of Figs. 2 and 3 shows that one can obtain values of the transmittance with errors less than the error in q--i.e., for values of $T_s > .6$; such is not the case for the values of the extinction coefficient. The least error in the estimate of the extinction coefficient is at best equal to and is generally greater than the error in q.

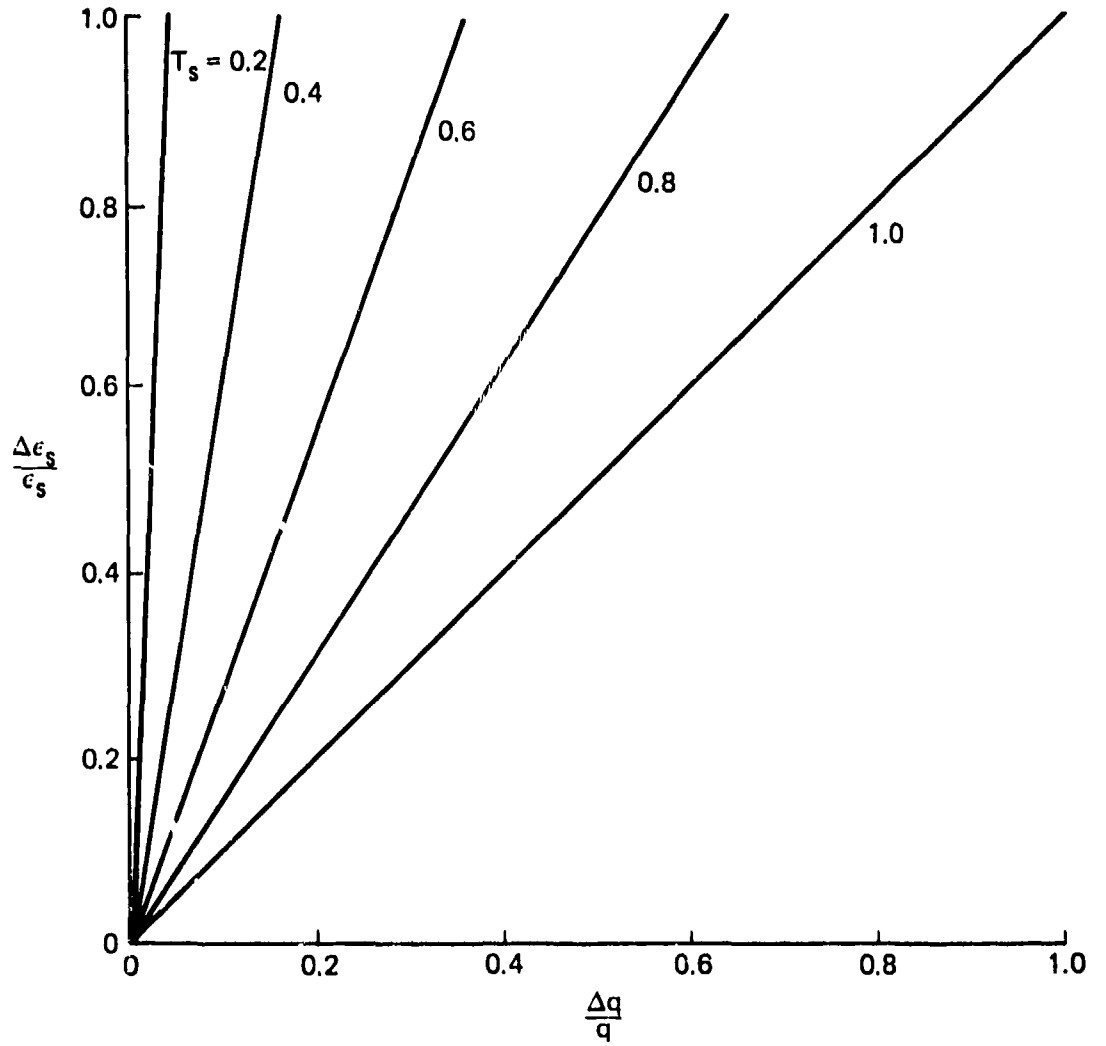

Fig. 3--Effect of error in q on estimated extinction coefficient

IV. OBSCURANT CONCENTRATION AND CL VALUES

With a functional value for the extinction coefficient and certain other parameters of the smoke constituents in a localized region of space, it is theoretically possible to infer the spatial concentration throughout the region of nonzero lidar return. To compute the concentration, set

$$\varepsilon_s(z) = \int_0^\infty dr\ n_s(r, z)\sigma_s(r) \tag{19}$$

and

$$C_{gs}(z) = \rho_0 \int_0^\infty dr\ n_s(r, z)\left(\frac{4\pi}{3} r^3\right) , \tag{20}$$

where $n_s(r, z)$ is the number of smoke particles of radius r at range z per unit volume, and $\sigma_s(r)$ is the extinction cross section for particles of radius r. The density of the smoke constituents is ρ_0 (in grams per cubic centimeter), where the smoke constituents are assumed approximately spherical. The total number of smoke particles per unit volume $N_s(z)$ at range z can be written

$$N_s(z) = \int_0^\infty dr\ n_s(r, z) . \tag{21}$$

Then

$$\varepsilon_s(z) = N_s(z)\langle\sigma_s\rangle \tag{22}$$

and

$$C_{gs}(z) = \rho_0 N_s(z) \langle v_s \rangle \ , \tag{23}$$

where $\langle \sigma_s \rangle$ is the average smoke extinction cross section and $\langle v_s \rangle$ the smoke particle volume for the distribution function $n_s(r, z)$. Let $k = \rho_0 \langle v_s \rangle / \langle \sigma_s \rangle$, so

$$C_{gs}(z) = k\varepsilon_s(z) \tag{24}$$

and

$$CL_s = \int_0^z dz' \ C_{gs}(z') = k \int_0^z \varepsilon_s(z') \ dz' \ . \tag{25}$$

To use the formulas for C_{gs} and CL_s necessitates estimating k for a localized region in the smoke cloud along the propagation path of the lidar beam, where values for $\varepsilon_s(z)$ can be calculated. There are two main methods of obtaining values for k. The first considers the various terms for k separately. For a known smoke cloud, since the material of the assumed single scattering component is known, ρ_0 is known. Then from local measurements of $n_s(r, z_0)$ and $\sigma_s(r)$, $\langle v_s \rangle$, $\langle \sigma_s \rangle$, and k can be calculated. In the second method, the value of k is found by making a direct measurement of C_{gs} at some z and dividing the value by $\varepsilon_s(z)$ at that point.

Accurate values for C_{gs} and CL_s require accurately measuring $n_s(r, z)$ and $\sigma_s(r)$ in the first method. However, accurate measurements of $n_s(r, z)$ seem quite difficult to obtain. For example, in the report from Smoke Week II [Farmer et al., 1979], comparison of data from a particle-sizing interferometer and the measurements made in the Signature Characterization Facility showed "radically different size distributions." Compounding the errors in $n_s(r, z)$ are those associated with uncertainties in ρ_0 and $\varepsilon_s(z)$.

A simple local measurement of C_{gs} is subject to minimal error; uncertainty in C_{gs} and CL_s at other ranges will be due mainly to the uncertainty in $\varepsilon_s(z)$. The second method of directly measuring the

mass concentration is therefore less prone to uncertainty than the first, but it can be improved by measuring $\varepsilon_s(z)$ along with $C_{gs}(z)$. That procedure will obtain a better value of C_{gs}/ε_s, as well as check the lidar model by comparing the calculated with the locally measured ε_s. A further improvement would be to take more than one local point measurement along the path of propagation, then use the data to verify the model; if the measurements showed variation from the model, the model assumptions could be modified.

In any case, it is clear from Eqs. (24) and (25) that *relative* values of the concentration and CL are obtained directly from the extinction coefficient. The relative values alone are useful for studying the spatial and temporal evolution of the obscurant cloud, even without an absolute calibration.

V. APPLICATION OF MODEL TO DATA

We applied the technique for calculating the various smoke cloud parameters outlined above to the 10.6 μm backscatter data (Fig. 1) and the transmittance measurements of event F-6 (where artillery shells were fired to produce a dust cloud) in the DIRT-I program [van der Laan, 1979]. The 10.6 μm backscatter data at T = 0 show the ambient air backscatter amplitude as a function of the range $P_a(z)$, where the two spikes are due to reflectors for distance calibration and transmittance measurements. At T + 19s the 2000 m target return is not visible. By T + 2 min, the target return is clearly visible, the cloud is still substantial, and there is a fairly good signal between the cloud and the target. Since we had a particle size distribution measurement from event F-6 at approximately T + 2 min [Loveland et al., 1979], the T + 2 min backscatter data were chosen for $P_c(z)$, so that $T_s(z)$ and $\varepsilon_s(z)$ as well as $C_{gs}(z)$ and $CL_s(z)$ could be calculated.

Equation (1) was used to obtain a theoretical curve fit to the ambient backscatter data (without the two spikes from the reflectors) $P_a(z)$. Employing Eq. (1) in the curve fit, the explicit expression for G(z) must be used, and we must assume a Gaussian aperture and field of view, as well as that the pulse is short and β_a and ε_a are constant. Several runs were made to obtain a curve fit to $P_a(z)$. The best fit is shown in Fig. 4, with results for the parameters $A\beta_a = 1.8 \times 10^6$, $\varepsilon_a = 1.1\ km^{-1}$, and b = 21.3 cm.

At close ranges, much of the backscatter is not collected by the receiver until the field of view overlaps the beam. That is because of the receiver/transmitter separation b and the associated field-of-view and beam divergence. Figure 4 shows that the backscatter power amplitude increases until it peaks (region of overlap of the field of view with the beam), thereafter monotonically decreasing with range--as expected. Figure 5 illustrates the beam and field-of-view overlap, with θ_t = 1.2 mrad and θ_r = 1.23 mrad; the overlap is at approximately z = 175 m, which is consistent with the peak shown at approximately 180 m in Fig. 4.

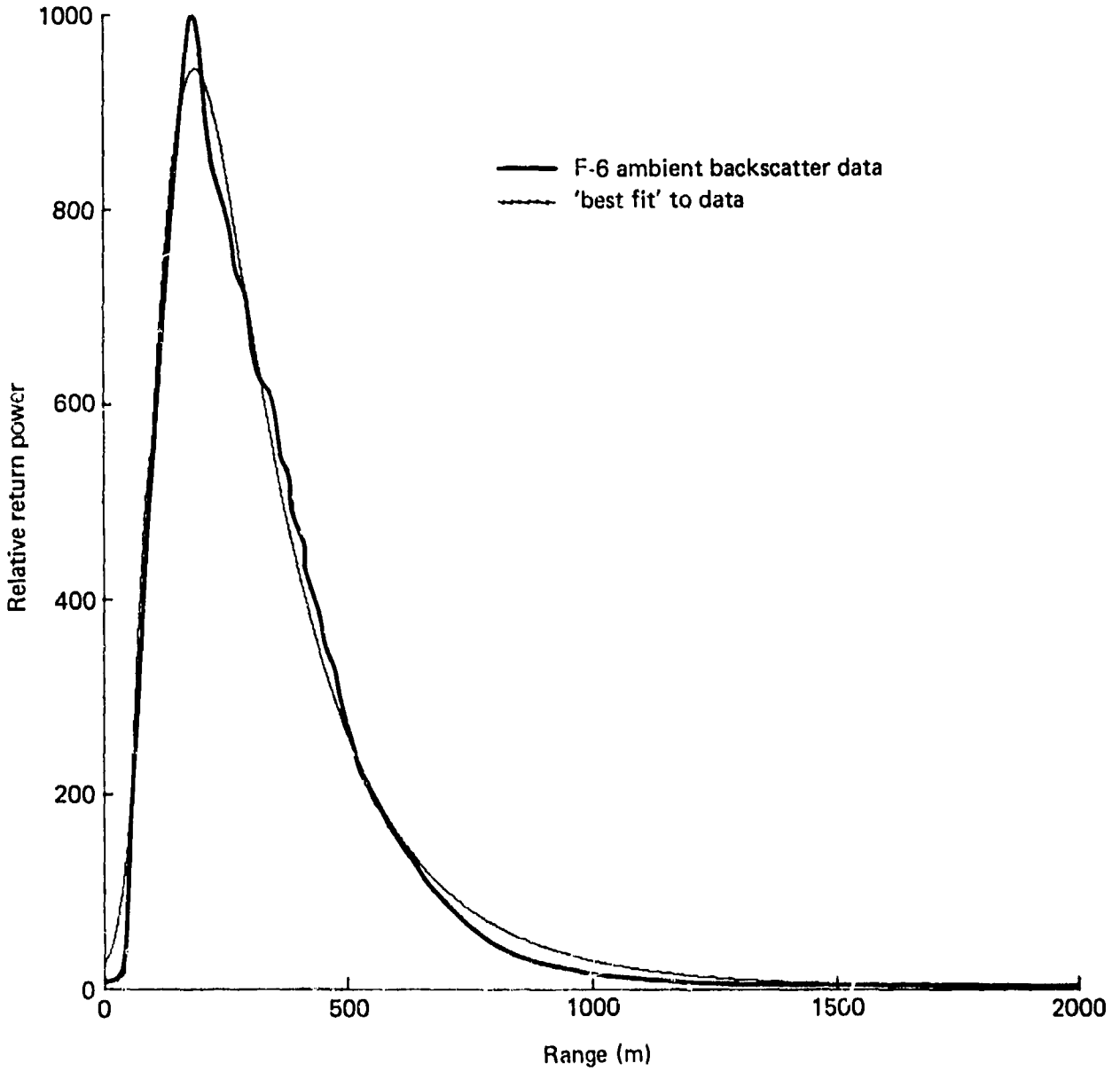

Fig. 4--Best fit to ambient backscatter data

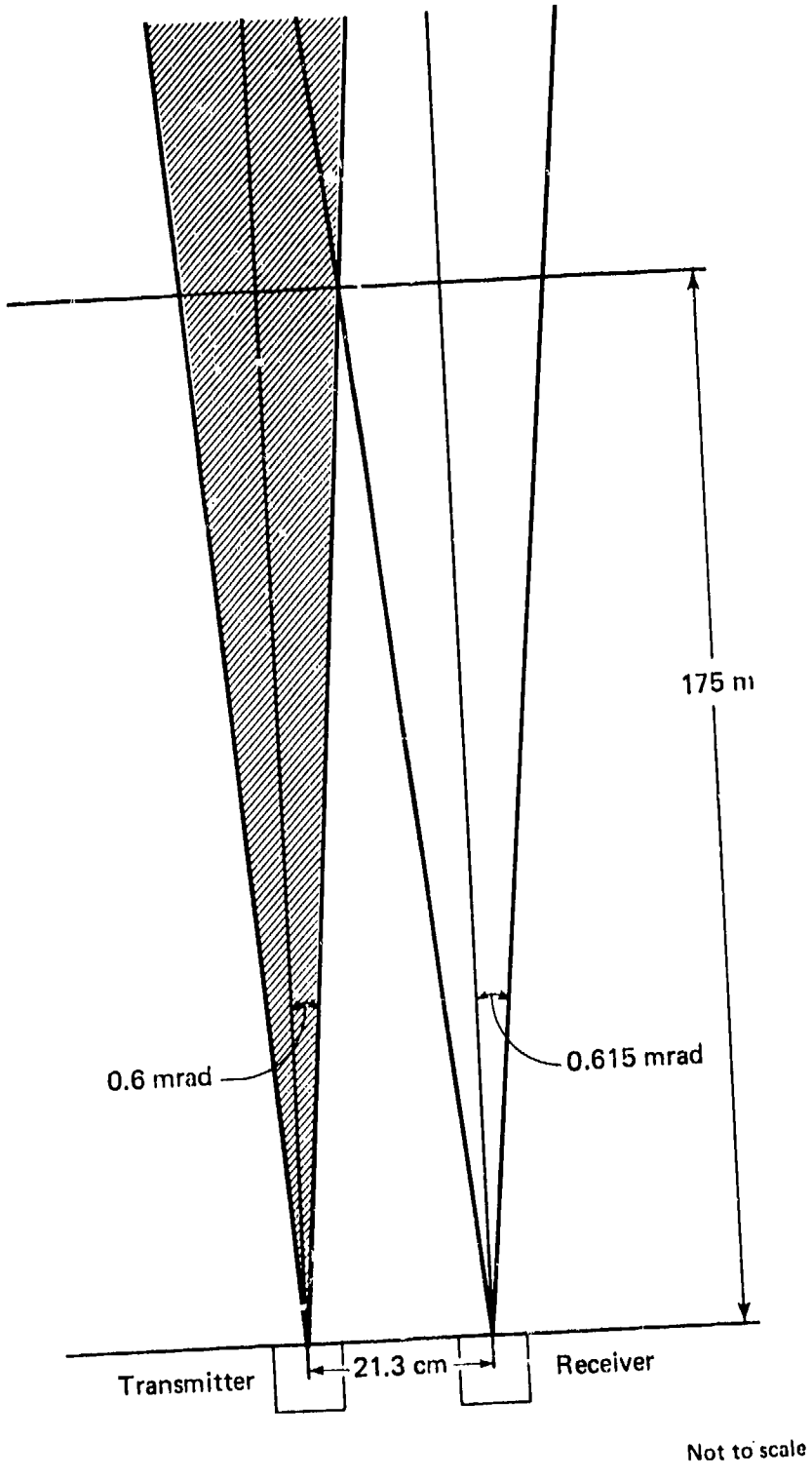

Fig. 5--Beam and field-of-view overlap

The first quantity calculated was the smoke transmittance. The ratio $P_c(z)/P_a(z)$ was known as a function of the range z from the backscatter data. A reasonable value for α_s ($\approx .015$) can be found from the results of Smoke Week II [Sztankay et al., 1979], but not for β_a. Method IIb was therefore applied to find a value of q. A relative target return transmission of $R_c/R_a = .74$ at a target range $z_t = 2000$ m was used to iterate for a value of q, using Eq. (13). ($R_c/R_a = .74$ is consistent with $P_c(z_t)/P_a(z_t) = .74$.) The value of q calculated by this method is 7.3×10^{-7} cm^{-1}; with $\alpha_s = .015$, β_a is 5.5×10^{-9} str^{-1} cm^{-1}. Substituting q into Eq. (13), the smoke transmittance can be estimated for all values of the range, with the results shown in Fig. 6. Figure 6 also plots T_s for $\Delta q/q \leq .1$ (dark shading) and $\Delta q/q \leq .5$ (diagonal shading), illustrating that the error in T_s is about half the uncertainty in $\Delta q/q$. Numerically, $\Delta T/T < .05$ for $\Delta q/q \leq .1$ and $\Delta T/T < .3$ for $\Delta q/q \leq .5$; the approximation to the error [Eq. (16)] gives a slight underestimate.

Once the smoke transmittance and q are known, using Eq. (14) to calculate $\varepsilon_s(z)$, the local value of the smoke extinction coefficient at range z, is quite simple. The value of ε_s is then substituted into Eq. (24) to derive the mass concentration. To calculate C_{gs} in absolute units, the value k must first be found.

The results of measuring the particle size distribution for event F-6 of DIRT-I, conducted at approximately T = 2 min, are reproduced in Fig. 7. The data are averages over a 10 sec interval; since the velocity of the probes was 10 m/sec, the range interval is 100 m (assumed to be in the center of the cloud z_c). The particle size distribution (for the smoke) $n_s(r, z_c)$ as estimated from Fig. 7, where r ranges from 1 - 200 μm, is

$$n(r, z_c) = \frac{3.4 \times 10^5}{r^{3.14}} \frac{(\mu m)^{2.14}}{\text{liter}} . \qquad (26)$$

Letting $\rho_0 = 2.5$ gm/cc, a value commonly used for dust [Patterson, 1977], and substituting that value and Eq. (26) into Eq. (20) results in a value for C_{gs} in the interval at z_c,

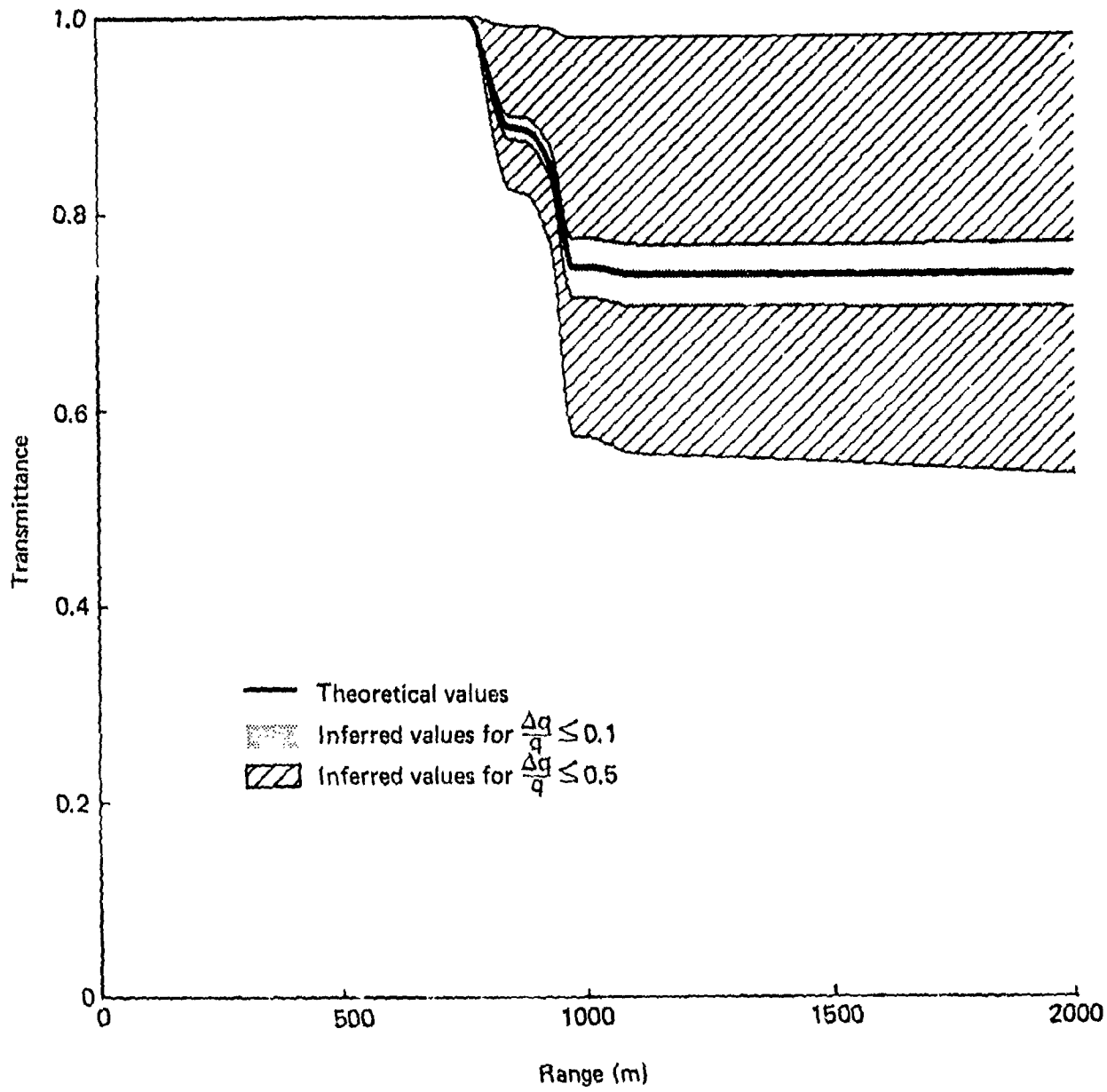

Fig. 6--Sensitivity of inferred transmittance to uncertainties in q

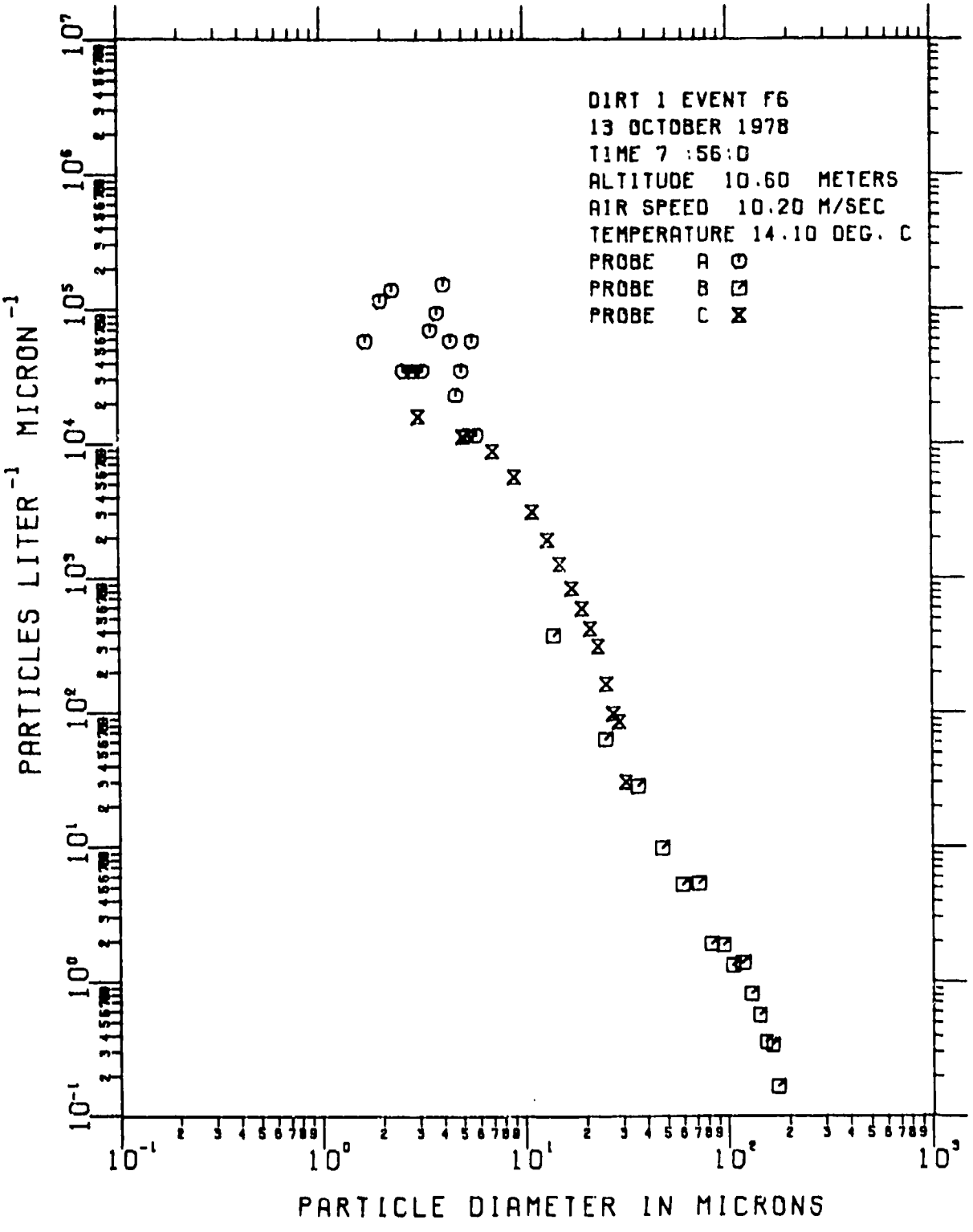

Fig. 7--Particle size distribution measurement for event F-6, DIRT-I

$$C_{gs}(z_c) = 3.8 \times 10^{-4} \text{ gm/liter} = .38 \text{ gm/m}^3 , \qquad (27)$$

which agrees with the dust results from Smoke Week II [Farmer et al., 1979]. The above value of C_{gs} is divided by an average smoke extinction coefficient in the interval about z_c to obtain

$$k = 9.6 \text{ cm-gm/liter} = 9.6 \times 10^3 \text{ cm-gm/m}^3 . \qquad (28)$$

The values of $C_{gs}(z)$ can be evaluated for the full range 0 to 2000 m. Figure 8 plots the calculations for the smoke extinction coefficient (scale on left side) and the smoke mass concentration (scale on right side), where scale for the range has been expanded. Also plotted are the uncertainties with $\Delta q/q \leq .1$ (dark shading) and $\Delta q/q \leq .5$ (diagonal shading). The numerical calculations show that for $\Delta q/q \leq .1$, $\Delta\varepsilon_s/\varepsilon_s$ is about .15 in the region of large ε_s--very close to the theoretical calculation [Eq. (18)] of about .14. The numerical analysis also confirms the theoretical prediction for the behavior of $\Delta\varepsilon_s/\varepsilon_s$ given small values of ε_s. $\Delta\varepsilon_s/\varepsilon_s$ may be as great as 10^4, but only when $\varepsilon_s << 1$; the plot confirms that such errors will not cause problems. For values of $\Delta q/q \sim .5$, errors in $\Delta\varepsilon_s/\varepsilon_s$ and $\Delta C_{gs}/C_{gs}$ are only on the order of 1.

As for the question of a local versus a particle distribution measurement of C_{gs}, consider the data for calculating $n_s(r, z)$ in Fig. 7. Choosing a straight-line log fit to the data is subjective; an analysis of the possible error shows that the range for k is about 27.8 to 1.9 cm-gm/liter--which translates to possible +190 percent to -80 percent errors in the calculation for C_{gs} before any errors due to Δq are considered. A direct local measurement of C_{gs} will significantly reduce such errors.

The final calculation is for CL_s [Eq. (25)], where the values of C_{gs} are substituted and the integration is carried out. The values for CL as a function of range are given in Fig. 9, showing also the uncertainty due to $\Delta q/q \leq .1$ and $\Delta q/q \leq .5$. Errors from $C_{gs}(z)$ propagate to errors in CL; added errors due to range are insignificant.

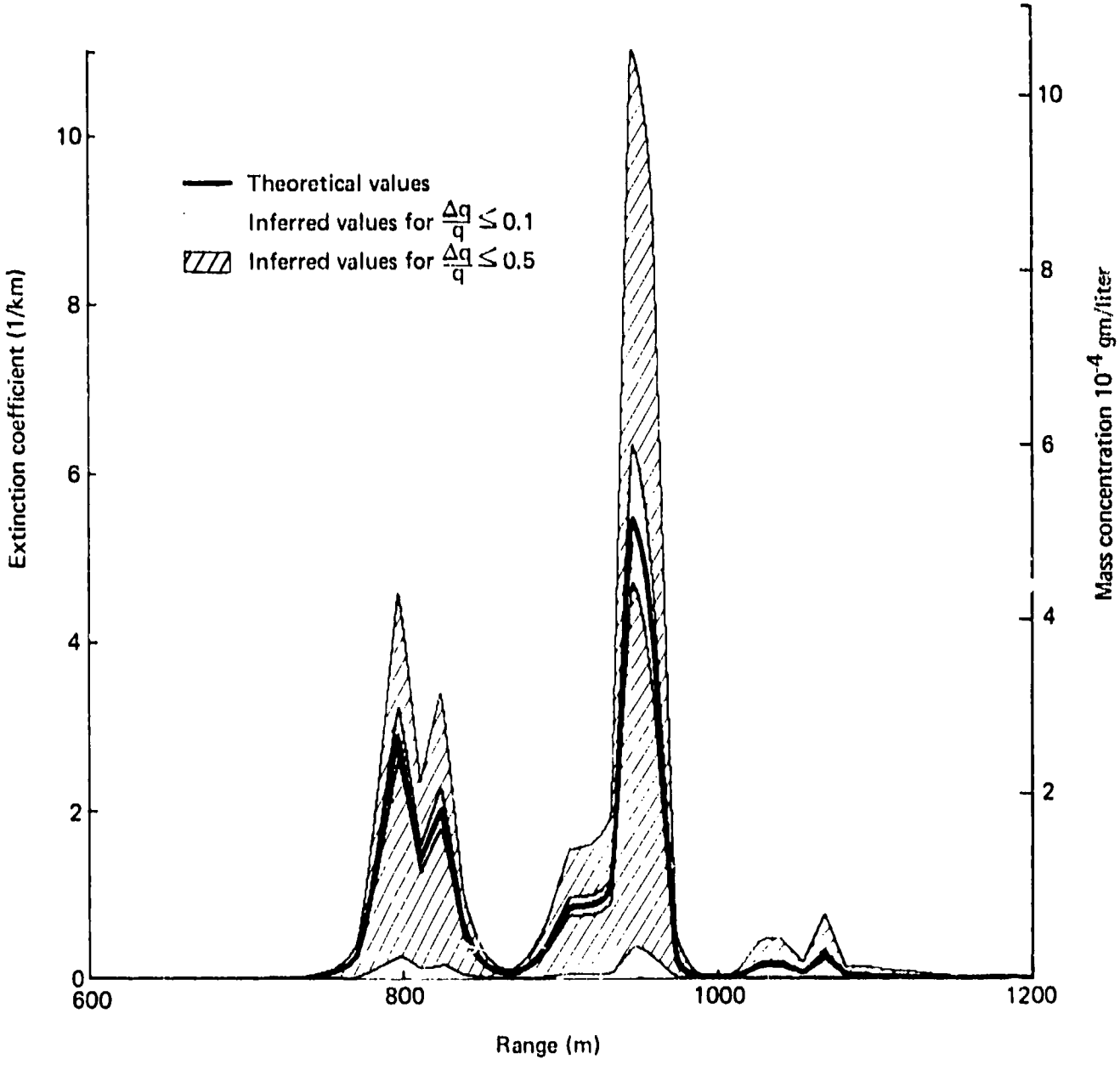

Fig. 8--Sensitivity of inferred extinction coefficient and mass concentration to uncertainties in q

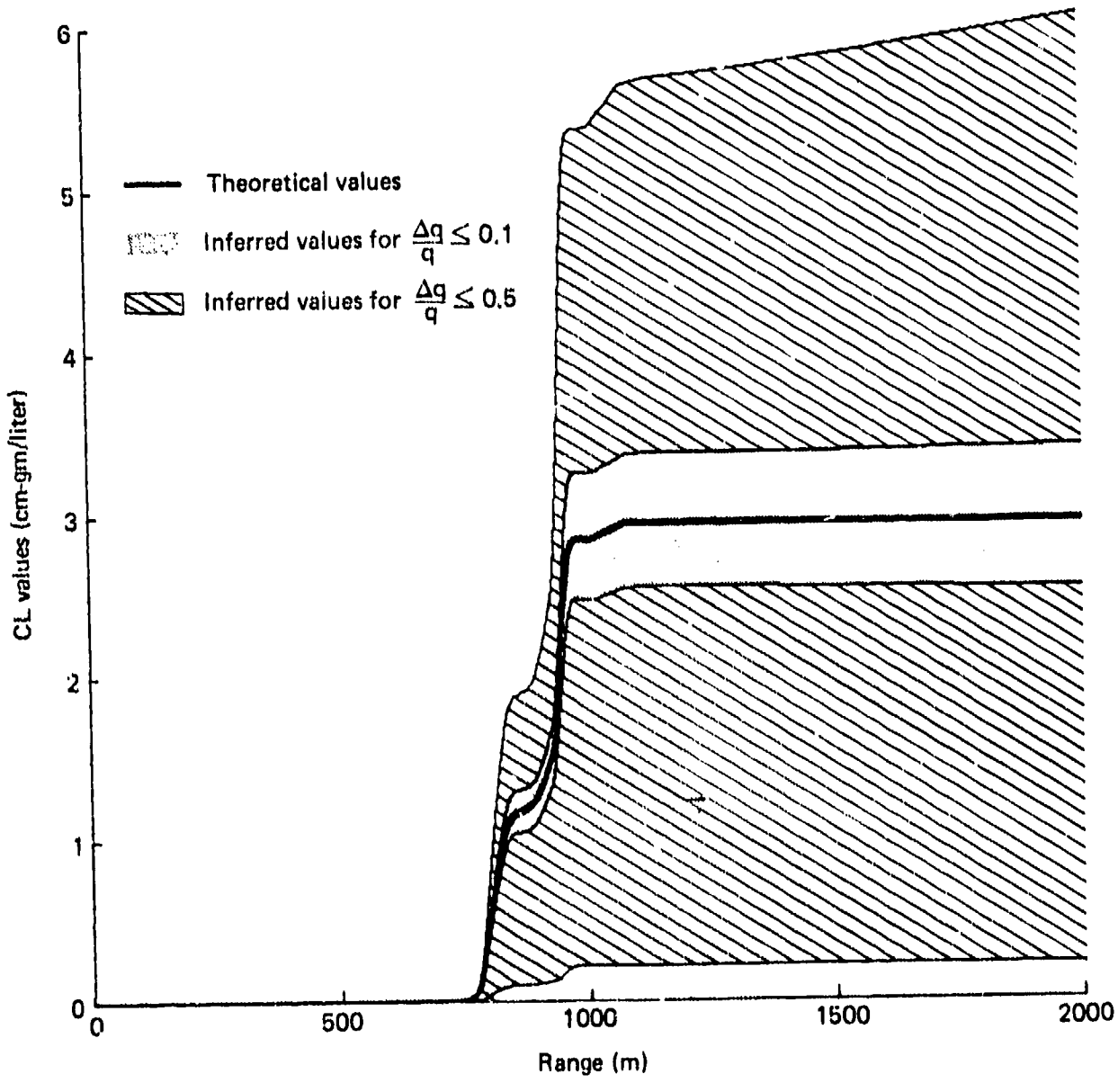

Fig. 9--Sensitivity of inferred CL values to uncertainties in q

VI. CONCLUSIONS

The analytic results show that with only lidar backscatter data, the transmittance and the extinction coefficient for smoke can be calculated. With a two-way smoke transmittance of .5, the estimated errors are $\Delta T_s/T_s \simeq .5\ \Delta q/q$ and $\Delta\varepsilon_s/\varepsilon_s \simeq 2\Delta q/q$; to achieve good estimates of ε_s, the uncertainty in q must therefore be minimized. To estimate the mass concentration and CL values in absolute units requires information on the obscurant particulates. The usual quantity measured is the smoke particle size distribution $n_s(r, z)$, but because of the difficulty of accurately measuring $n_s(r, z)$ and the compounded errors from other measurements needed to calculate k (the ratio of mass concentration to extinction coefficient), we argue in favor of a direct local measurement of C_{gs}. A point measurement of ε_s would further decrease the uncertainty in k. Additional local measurements at different ranges within the smoke cloud would yield information to verify the model. Figure 10 diagrams the analysis.

Data for event F-6 of DIRT-I give quantitative results for $T_s(z)$, $\varepsilon_s(z)$, $C_{gs}(z)$, and $CL_s(z)$. The results show maximum errors of less than 5 percent in $T_s(z)$ and less than 20 percent in $\varepsilon_s(z)$ for $\Delta q/q = .1$. For the same value of $\Delta q/q$, the errors in $C_{gs}(z)$ and $CL_s(z)$ were less than 20 percent and 12 percent, respectively. However, estimates show a possible 200 percent additional error due to the uncertainty in $n_s(r, z)$ and ρ_0, used to estimate k in calculating C_{gs} and CL_s. Such a large error would not occur with a local measurement of C_{gs}.

To summarize, the principal conclusions of the study are that

- The inversion algorithm can produce reliable estimates of smoke or dust transmittance and extinction from all points within a cloud for which a resolvable signal can be detected.
- A single point calibration measurement can convert extinction values to mass concentration for each resolvable signal point.
- Having a target behind or to the side of the obscurant cloud aids in normalizing the transmittance and extinction estimates.

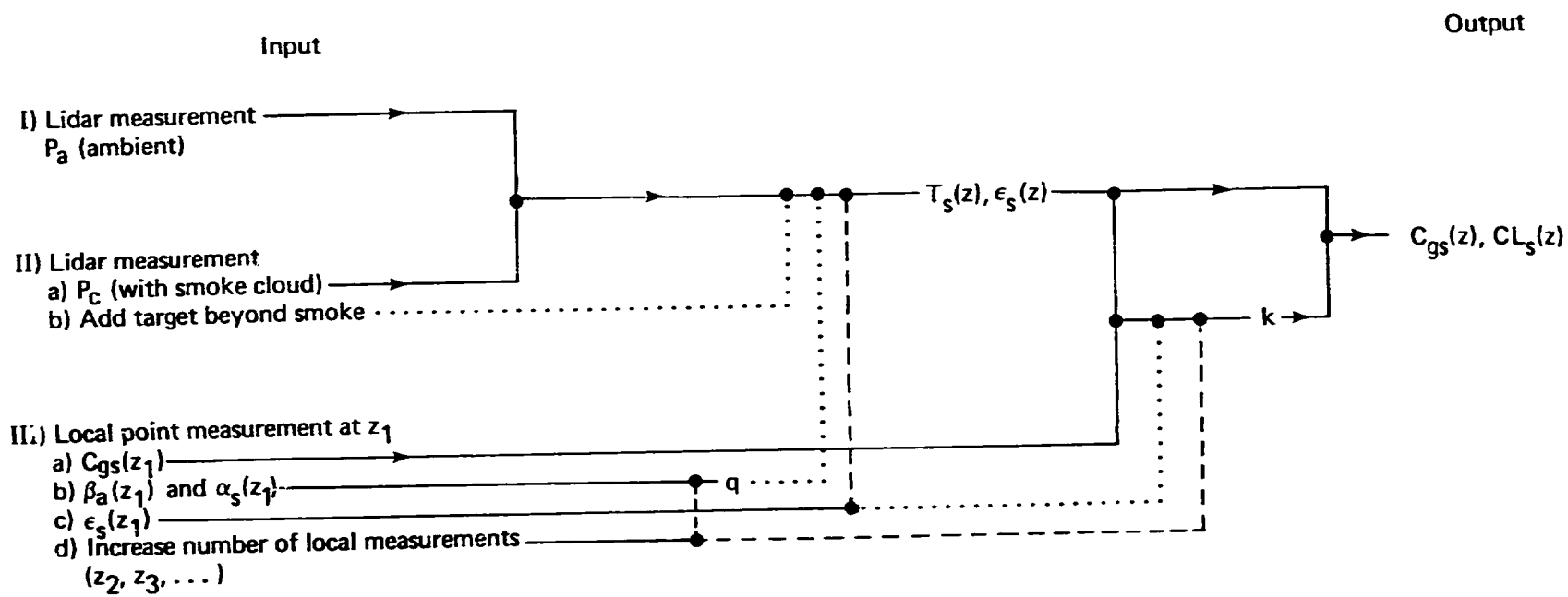

Fig. 10--Diagram of theoretical analysis. Logical flow of calculation of mass concentration and CL values using lidar.

APPENDIX

From Eq. (2), it is obvious that T_s^2 is bounded by 0 and 1; but in the final expression for T_s^2 [Eq. (13)], such is not the case. The problem arises in Eq. (12), where all the terms seem to take on arbitrary values. Physically, $P_c(z)$, $P_a(z)$, $\beta_s(z)$, β_a, and α_s must be greater than or equal to zero. Those conditions impose a set of inequalities given by

$$1 + \frac{\alpha s}{2\beta_a}\left(-\frac{dT_s^2(z)}{dz}\right) \geq \frac{P_c(z)}{P_a(z)} \geq \frac{\alpha s}{2\beta_a}\left(-\frac{dT_s^2(z)}{dz}\right)$$

for all z. If the lidar equation [Eq. (1)] accurately describes the backscatter power P_c and P_a, and if the assumed linearity between backscatter and extinction is valid, the above inequality will always hold for true data. Therefore, the solution to Eq. (12) will yield values of T_s^2 between zero and 1. For real data, there is noise in P_c and P_a and uncertainty in the true values of β_a and α_s, so a minor violation of the inequality is not sufficient to invalidate the equations or the assumptions.

REFERENCES

Farmer, W. M., et al., *Interferometric Particle Size Measurements during Smoke Week II*, University of Tennessee Space Institute, 1979.

Fenn, R. W., "Correlation between Atmospheric Backscattering and Meteorological Visual Range," *Appl. Opt.* 5, 1966, pp. 293-295.

Loveland, R. B., et al., "Particle Size Distribution Measurements," Chap. 9 in J. D. Lindberg (compiler), *Measured Effects of Battlefield Dust and Smoke on Visible, Infrared, and Millimeter Wavelength Propagation: A Preliminary Report on Dusty Infrared Test-I (DIRT-I)*, U.S. Army Electronics Research and Development Command, Atmospheric Sciences Laboratory, Report ASL-TR-0021, January 1979.

Patterson, E. M., "Atmospheric Extinction between 0.55 μm and 10.6 μm Due to Soil-Derived Aerosols," *Appl. Opt.* 16, 1977, pp. 2414-2418.

Sztankay, Z. G., et al., "Backscatter and Extinction Measurements at Smoke Week 2," U.S. Army Electronics Research and Development Command, 1979.

van der Laan, J. E., *Lidar Observations at 0.7 μm and 10.6 μm Wavelength during Dusty Infrared Test I (DIRT-I)*, U.S. Army Research and Development Command, Atmospheric Sciences Laboratory, Report ASL-CR-0001-2, September 1979.

Warren, R. E., and R. F. Lutomirski, *Analysis of Lidar Utility for Characterizing Battlefield Environments*, Pacific-Sierra Research Corporation, Report 912, May 1979.